Anesthetic Interaction with Ketosteroid Isomerase: Insights from Molecular Dynamics Simulations

Michael J. Yonkunas,* Yan Xu,*† and Pei Tang*†
Departments of *Anesthesiology and †Pharmacology, University of Pittsburgh School of Medicine, Pittsburgh, Pennsylvania

ABSTRACT The nature and the sites of interactions between anesthetic halothane and homodimeric Δ^5-3-ketosteroid isomerase (KSI) are characterized by flexible ligand docking and confirmed by ^1H-^{15}N NMR. The dynamics consequence of halothane interaction and the implication of the dynamic changes to KSI function are studied by multiple 5-ns molecular dynamics simulations in the presence and absence of halothane. Both docking and MD simulations show that halothane prefer the amphiphilic dimeric interface to the hydrophobic active site of KSI. Halothane occupancy at the dimer interface disrupted the intersubunit hydrogen bonding formed either directly through side chains of polar residues or indirectly through the mediation of the interfacial water molecules. Moreover, in the presence of halothane, the exchange rate of the bound waters with bulk water was increased. Halothane perturbation to the dimer interface affected the overall flexibility of the active site. This action is likely to contribute to the halothane-induced reduction of the KSI activity. The allosteric halothane modulation of the dynamics-function relationship of KSI without direct competition at the enzymatic active sites may be generalized to offer a unifying explanation of anesthetic action on a diverse range of multidomain neuronal proteins that are potentially relevant to clinical general anesthesia.

INTRODUCTION

It is still under debate where and how general anesthetics interact with proteins in the central nervous system (CNS) and consequently change the functions of these proteins (1). High-resolution structures are generally not available at this time for the potential anesthetic targets in the CNS implicated by the sensitivity measurements (1). The attempt to directly determine the anesthetic interaction with these proteins at atomistic resolution has therefore been severely hampered. Although some anesthetic-sensitive soluble proteins, such as firefly luciferase (2) and bovine or human serum albumin (3,4), do not exist in the CNS, the interaction of general anesthetics with these model proteins has been characterized extensively, and the information derived from these studies have provided valuable insights into the molecular mechanisms of general anesthesia.

Homodimeric enzyme, Δ^5-3-ketosteroid isomerase (KSI), can serve for the same purpose. KSI has been the subject of intensive studies in the past because of its proficient catalytic function for the isomerization of 3-oxo-Δ^5-steroids to their Δ^4-conjugated isomers and its role as a prototype for understanding the enzyme mechanism of the allylic rearrangement (5–8). The high resolution three-dimensional structure of KSI has been solved by nuclear magnetic resonance (NMR) and x-ray crystallography. Each subunit of KSI is composed of three α-helices and a six-strand mixed β-pleated sheet, which contains three β-bulges. The three α-helices and the back of the β-sheet form an active-site cavity that has a size of 8.5 Å by 9.5 Å at the surface and 16 Å deep (6). The active site cavity is lined mainly with hydrophobic residues. The residues located at the bottom of the active site, including Asp-38 and Tyr-14 as well as Asp-99 (6), are involved in forming hydrogen bonds to carbonyl oxygen of the steroid and are critical for the catalytic function of KSI. Another feature of KSI structure is that the fronts of the β-sheets from two subunits face each other in an antiparallel fashion to form the dimeric interface. Such structural arrangement appears to be a general scaffold for an active-site cavity that binds hydrophobic substrates and is essential for KSI function. Perturbations to the dimeric interface, such as mutating polar residues to nonpolar residues and consequently altering the geometry of the active site, have shown to lead to great decreases in the catalytic activity and conformation stability of KSI (9). The diversity in the secondary structural components, the elegant folding in the tertiary structure, and the distinct arrangement in the quaternary structure make KSI a good model system for other biological studies. Experimentally, we have confirmed (10) that i), anesthetic halothane could reduce KSI enzymatic activity; ii), NMR chemical shifts of many residues on the β-sheet of KSI could be perturbed by halothane in a concentration-dependent manner; and iii), direct NOE crosspeaks between halothane and several residues could be observed. In this study, the interaction sites of halothane with KSI were identified using the AutoDock program (11) and compared with the NMR results. Subsequently, five parallel 5-ns molecular dynamics (MD) simulations were carried out on fully hydrated KSI systems in the presence and absence of halothane to investigate the molecular details of anesthetic-protein interactions

Submitted March 23, 2005, and accepted for publication July 14, 2005.

Address all reprint requests to Professor Pei Tang, PhD, W-1357 Biomedical Science Tower, University of Pittsburgh School of Medicine, Pittsburgh, PA. Tel.: 412-383-9798; Fax: 412-648-9587; E-mail: tangp@anes.upmc.edu.

0006-3495/05/10/2350/07 $2.00

doi: 10.1529/biophysj.105.063396

and to shed light on how such interactions induce dynamics changes that might be significant to KSI function.

MATERIALS AND METHODS

System preparations

The NMR structure of homodimer KSI from *Comamonas testosteroni* (125 amino acids in each subunit) was obtained from the Protein Data Bank (1BUQ) (7). The structure was imported into AutoDock 3.0 (11) as a fixed protein, onto which a grid matrix box with 127 points and 0.375Å spacing resolution along X, Y, and Z dimension was placed at the center of mass of KSI. Halothane molecules were docked to KSI using the Lamarckian genetic algorithm supplied by AutoDock. The previously optimized geometry, atomic charges, and nonbonded interaction parameters of halothane (12,13) were used in this study. Docking parameters were adopted from an efficient docking procedure (14). Favorable docking results were determined on the basis of low docking energy and high occupancy. Four final halothane docking configurations, as shown in Fig. 1, were identified from the docking results as well as the chemical shift perturbation of KSI by halothane in the NMR measurements (10).

Five systems were prepared for MD simulations, including i), no halothane and no substrate; ii), only one halothane at the highest occupancy site at the center of the dimeric interface; iii), four halothane molecules at the four high-occupancy sites; iv), the same four halothane molecules, but in the presence of steroid substrate analog 19-nortestosterone hemisuccinate (19-NTHS) at the active sites; and v), only 19-NTHS at the active sites in the absence of halothane. The systems were fully hydrated using Solvate 1.0 (http://www.mpibpc.gwdg.de/abteilungen/071/solvate/node2.html). In addition to 6,917 TIP3 waters, 16 sodium ions and 8 chlorine ions were added to each system to provide 100 mM salt concentration and to neutralize the charges in the system.

Molecular dynamics simulations

All simulations were performed using the NAMD2 program (15) on the Cray T3E parallel computer and the HP alpha server GS1280 (JONAS) at the Pittsburgh Supercomputing Center. The CHARMM27 parameter set was used for the simulations. A conjugate gradient energy minimization with 10,000 steps was performed on each system, whereas the protein backbone was restrained with a harmonic force of 999 kcal/mol/Å^2. The systems were then subject to a NVT (constant number of atoms, volume, and temperature) equilibration at temperature of 300 K for 1.2 ns, during which the restraints on KSI backbone were reduced in a stepwise fashion from 999 to 0 kcal/mol/Å^2. Subsequently, 5 ns NPT dynamics simulations were carried out in parallel for the systems in the absence and presence of halothane. Langevin dynamics and Langevin piston pressure (16) were used to maintain temperature and pressure at 300 K and 1 bar, respectively, with a damping coefficient of 10 ps^{-1}. Periodic boundary conditions and continuous water and halothane wrapping were imposed. The SHAKE algorithm was set to restrain all hydrogen-parent bonds to an allowed tolerance of 10^{-5} Å. A time step of 1 fs was used, and energies and trajectories were recorded every 0.5 ps. Van der waals cutoff distance was 12 Å with the pair list distance extended to 13 Å. The long-range full electrostatic interactions were updated every four time steps by using the Particle Mesh Ewald (PME) method. Most of the data process and analysis were accomplished within the VMD 1.8.1 software environment (17).

RESULTS AND DISCUSSION

Halothane distribution in and around KSI

Four preferred halothane docking positions in KSI, as shown in Fig. 1, were initially identified by the halothane occupancies (the number of ligands docked at the same site during 100 trials) and by the docking energies (summation of internal energy of ligand and the intermolecular energy). More detailed docking information is summarized in Table 1s in the online supplemental materials. These docked positions were also verified experimentally with the high resolution NMR study (10), in which significant chemical shift changes and NOE crosspeaks were observed for the residues that are modulated by the presence of halothane molecules. The halothane molecules were numbered 1–4 based on the order of their docking energies (−4.32, −4.12, −4.10, and −3.84 kcal/mol). Variation of the internal energy of halothane is within ±0.02 kcal/mol; therefore, the difference in docking energy results mainly from the interaction of halothane with the surroundings of its docked positions. The middle of the dimeric interface, where halothane No. 1 is located, has the lowest docking energy and the greatest occupancy numbers, suggesting that the site is highly favorable for halothane. The disassociate constant, K_d, of halothane No. 1 was estimated to be ~1 mM on the basis of the binding energy (see detailed K_d calculations in the supplemental materials), which is defined in AutoDock as the summation of the torsional free energy and the intermolecular energy. Consistent with the result of binding energy, the trajectory of

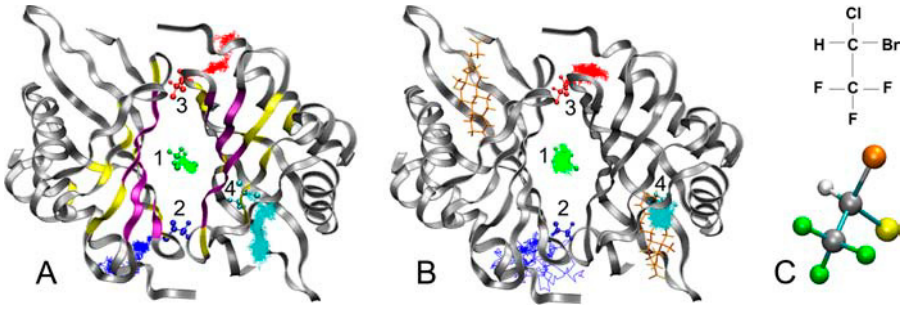

FIGURE 1 (*A*) Halothane motion trajectories over the 5-ns all-atom simulations in a fully hydrated KSI (system C). For clarity, water molecules are not shown. The initial positions of halothane are marked by their CPK representations. The residues whose chemical shifts are affected by halothane in NMR experiments are highlighted either in purple (strongly) or yellow (weakly). Notice reasonably good overlap between the halothane trajectories and halothane-perturbed chemical shift regions. System B contains only a single halothane molecule at location No. 1. (*B*) System D, where both subunits have a bound substrate analog 19-NTHS in the active site. Notice that halothane No. 4 has a much more restricted motion trajectory compared to that in system C. (*C*) Chemical structure of a halothane molecule.

halothane No. 1 showed very limited displacement over the course of 5-ns MD simulations. A similar halothane trajectory was obtained in a separate 5-ns MD simulation on system B, where there was only one halothane molecule at the dimer interface. In contrast, the outer edge of the interfacial region having slightly higher docking energies and significantly lower occupancy numbers could not tightly hold the two docked halothane molecules (Nos. 2 and 3). Halothane Nos. 2 and 3 seemed to interact with KSI less tightly and moved away from their initial positions relatively quickly. Each subunit of KSI forms a conical closed barrel with an open end that is the entrance of a hydrophobic cavity for substrate binding. Regardless of whether or not it was occupied by 19-NTHS, the active sites attracted at most one halothane molecule at its entrance, shown as halothane No. 4 in Fig. 1 *A*. A smaller displacement range of the motion trajectories for halothane No. 4 was observed when the active site was occupied by 19-NTHS, as depicted in Fig. 1 *B*, presumably because halothane resided in a much more restricted space and interacted more effectively with the surrounding residues.

A strong preference for the dimer interface and less attraction to the active-site cavity of KSI underscored the molecular characteristics of halothane in defining the anesthetic interaction site. Hydrophobic and hydrophilic residues at the long patch of the β-sheet of each subunit forms a narrow amphiphilic ''tunnel'' at the dimeric interface, where a few water molecules were ''trapped''. The active site, however, is mainly surrounded by the apolar residues that largely block the access of water molecules, even though the wide-opened entrance of the active site are facing bulk water. The motion trajectory of halothane No. 4 in Fig. 1 showed that this molecule moved neither into the bulk water nor inside of the cavity where long-lasting presence of water could not survive, revealing the predominantly amphiphilic nature of halothane molecules.

The KSI residues in the regions where halothane molecules were initially docked by AutoDock or later sampled in MD simulations coincided with those whose chemical shifts were perturbed by halothane molecules in the NMR experiments, as highlighted in Fig. 1 *A*. A full description of the NMR study will be reported elsewhere.

Halothane effects on the dimer interface

The importance of the dimer interface to the function of KSI has long been recognized. The stability of the interface is achieved by electrostatic and hydrophobic interactions between the side chains in different subunits (18). Among several potentially interacting residues, two pairs of electrostatic interactions were observed in the early stage of MD simulations. The polar interactions between the carboxylate of E70 and the amine of N120 did not last long, whereas the salt bridge between E77 and R113 in the control system remained strong for the entire duration of simulations, as depicted in Fig. 2. These long-lasting electrostatic interactions between carboxylate oxygens of E77 of one subunit and the side-chain amine of R113 of the other subunit, however, were disrupted in systems that bear a halothane molecule at the dimer interface. As halothane moved near E77 or R113, it distracted the side-chain orientation of E77 or R113 such that the interactions between the side chains were affected. It was noticed that the halothane effect on the E77-R113 salt bridge could only be imposed onto the pair in the immediate vicinity of the halothane molecule and not the other pair remote from halothane. MD simulations in all three systems (B–D) generated similar results and confirmed that a single halothane molecule could affect quaternary interaction by weakening the salt-bridge at the dimer interface without high-affinity binding.

The observation of strong halothane perturbation on E77 and R113 in MD simulations was verified by significant NMR chemical shift changes in both side chains of E77 and R113 after the addition of halothane. Moreover, a positive ^{1}H NOE crosspeak between halothane and $^1H_\beta$ of E77 was identified in NMR NOESY spectra, confirming unambiguously that halothane and E77 were close in space and that the halothane tumbling rate near E77 was slow.

Perturbation to the quaternary structure of KSI through the weakening of salt bridges and polar interaction at the dimer interface may directly impact KSI's biological function. The importance of dimerization in the formation and maintenance of the functional native tertiary structure of KSI has been discussed previously (19). The dimeric interactions mediated by charged and polar residues R72, N120, and E118 were manipulated by single-point mutation with the apolar amino acid alanine in the homologous KSI from *Pseudomonas putida* (9). Because one side of the active-site cavity is lined with residues from the ''front face'' of the

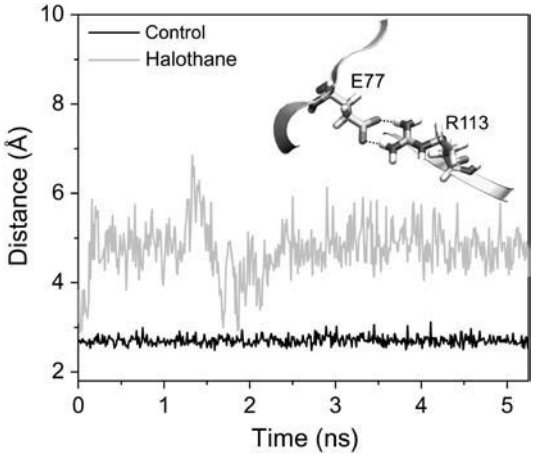

FIGURE 2 Electrostatic interactions between residues E77 and R113 at the dimer interface of KSI. The distances from the carboxylate oxygen of E77 of subunit A to the side-chain amine of R113 of subunit B, or vice versa, in the presence (*shaded*) or absence (*solid*) of halothane, are plotted as a function of simulation time.

interfacial β-sheet, such alteration to the charged residues at the dimer interface affected not only the salt bridges and water behaviors at the interface, but also the geometry of the active site. Consequently, the modification at the dimer interface resulted in profound reduction in the conformational stability as well as the catalytic activity of KSI enzyme activity (9).

Halothane effects on water at the dimeric interface

Bound water molecules at the protein surface or its interior could impose a determinant influence on protein function. A string of 10 bound water molecules was found in the middle of the dimeric interface in the crystal structure of KSI from *Pseudomonas putida* (5). Similar numbers of bound water molecules were also found in these MD studies. On average, there were a total of 9–10 and 6–7 ''bound'' waters at the dimeric interface in the absence and presence of halothane, respectively. A lesser number of bound water molecules in the systems with halothane can be probably attributed to a smaller free space due to halothane occupancy at the dimer interface. In addition to the difference in the total number of bound water molecules at the interface, a more important distinction of the bound water between the systems with and without halothane is the exchange rates between the bound water and the free bulk water. For an arbitrary given time point in MD simulations, the bound water molecules were identified and registered. The locations of these registered water molecules were monitored in the subsequent simulations. As shown in Fig. 3, the number of registered bound water molecules was reduced in a single exponential decay as a function of the simulation time; the decay was significantly faster for the system with halothane. This faster water exchange at the interface can change the dynamic characteristics of the dimer. Data collected at different selected time points provided similar fitting results as shown in Fig. 3. The average residence times of bound water molecules are 273.4 $\pm$ 96.0 ps and 401.4 $\pm$ 86.3 ps for the systems with and without halothane, respectively, in excellent agreement with the experimentally measured residence timescale (100–1000 ps) for strongly bound waters in proteins (20,21).

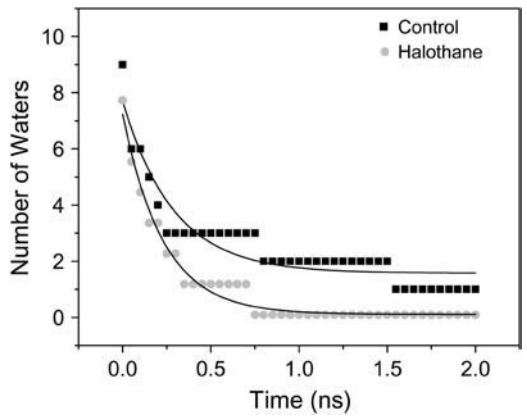

FIGURE 3 Halothane effects on water behavior at the dimer interface of KSI. The number of water molecules at the interface at an arbitrarily defined time point was counted and the identity of these water molecules was registered. The number of these registered water molecules was plotted as a function of subsequent simulation time and the data were fit using a single exponential decay function. The decay of the number of registered water along the simulation time reflects the exchange rate of the bound water with the bulk water. Halothane accelerates the apparent water exchange rates.

It is worth mentioning that some of the bound water molecules mediate intersubunit hydrogen bonds. One particular water molecule resides at the same location for the entire 5-ns simulation and formed three hydrogen bonds, two with Nε_2 of H100 in the two subunits and one with Hη_{21} of R113. This three-way hydrogen bonding generated great stability for the bound water as well as for the dimeric structure. The rest of the bound water molecules either involved in bridging hydrogen bonds between subunits or formed small water clusters through their own hydrogen bonding. The formation of water clusters at the dimer interface is consistent with the observations in other protein cavities studied by experiments (22) and by MD simulations (23).

The effects of halothane on the bound interfacial waters are evidenced by the decreasing number of bound waters and shortening of water residence time in the presence of halothane. Direct halothane interaction with side chains of polar residues at the dimer interface may have modified the overall contact between two subunits, altered the motion of the interfacial region (as discussed in the following section), and consequently affected the active site and enzymatic function. The thermodynamic consequences of disrupting a water-mediated hydrogen bond network in proteins by ligands can be enthalpically unfavorable, but entropically favorable (24). The enthalpy-entropy compensation is believed to be a general feature for many intermolecular interactions (25).

Halothane effects on the KSI structure and dynamics

Structural stability and flexibility of KSI over the course of MD simulations were evaluated by the root mean-square deviations (RMSD) and the root mean-square fluctuations (RMSF) of the backbone C_α. As shown in Fig. 4, RMSD values were over 1 Å after more than 1 ns restrained MD simulations and continued to increase at the beginning of the 5-ns free MD simulation. Plateaus were reached after 1.5–2 ns unrestraint simulations for individual subunits and the dimer structure. In agreement with previous studies (26,27), subunit B seemed slightly more stable than subunit A. Similar results were obtained for systems in the presence of 19-NTHS. Overall C_α RMSD revealed no significant difference in the KSI structure in the presence and absence of halothane molecules, which is consistent with our earlier assertion from experimental and computational studies (28,29) that anesthetic molecules often have negligible effects on protein structures.

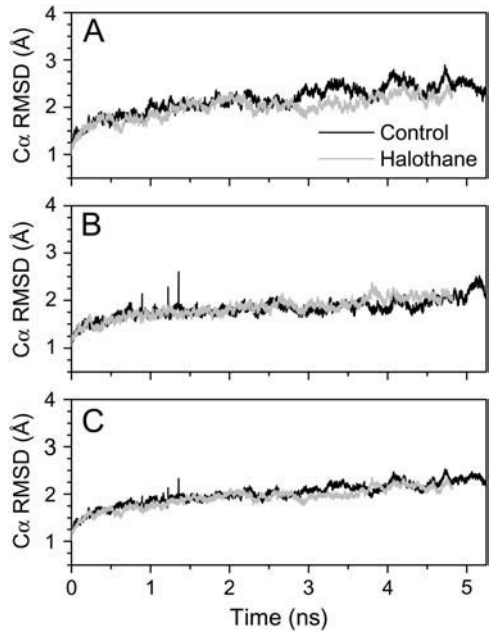

FIGURE 4 Comparison of structural drift revealed by the root mean-square deviation of the C_α atoms in the control system (*solid*) and the system having 4 halothane molecules (*shaded*) over the duration of 5-ns MD simulations: (*A*) subunit A, (*B*) subunit B, and (*C*) average for both subunits.

Fluctuations in the amplitude of RMSF correlated very well with KSI secondary structural elements, as depicted in Fig. 5. Significantly higher RMSF values are found in turns and loop regions, whereas relatively lower RMSF values are associated with helices and β-strands. The outermost turn, involving Q89 and G90 and connecting β4 and β5, exhibits the largest RMSF in both systems with and without halothane. The turns of the β-strands seem to experience more dynamic motions than those loops linking the α-helices, whereas the β-strands seem to be more rigid and possess smaller RMSF values than the helices. This combination of flexible and rigid elements of structure ensures KSI to perform its functions while maintaining a stable structure.

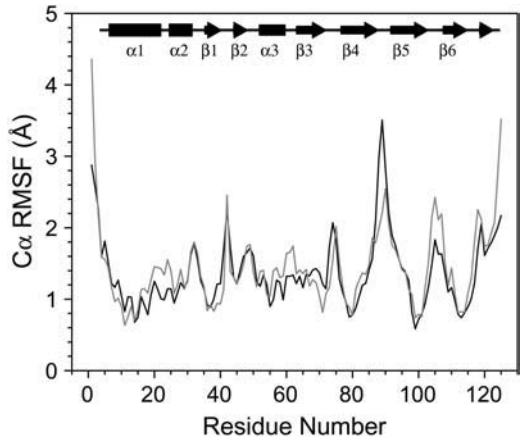

FIGURE 5 Structural flexibility shown as the root mean-square fluctuations of the C_α atoms in system A (*solid*) and system C (*shaded*) from the last 3 ns of simulations.

The effects of halothane on dynamics of KSI can be visualized in Fig. 5. The overall RMSF patterns are similar in the presence and absence of halothane, indicating similar motional profiles. In the presence of halothane, however, β4, β5, and β6 strands, where many residues reside within 3 Å from halothane No. 1, showed slightly higher RMSF, and the regions extending from the end of α1 to α3 exhibited a larger increase in RMSF. The changes in RMSF in these two regions are nevertheless different. Whereas the small RMSF increase in β4, β5, and β6 strands occurred mostly within the strands, the large RMSF increase from the end of α1 to α3 is predominantly caused by the profound changes in the fluctuations leading to and within the loops linking the various secondary structural components. It is almost certain that the primary cause for the increased flexibility in the region from the end of α1 to α3 is not due to the presence of halothane No. 4 at the entrance of the active site, because a similar RMSF increase occurs in the same region in system B, where there was only one halothane at the dimer interface and no halothane at the entrance of the active site. The RMSF increase in the regions from the end of α1 to α3, even in system B with only one halothane at the dimer interface, suggests that the halothane perturbation to the interface propagated through the tertiary folds around the active site. It is conceivable that the altered flexibility in the loops linking α1 to α2, α2 to β1, and β2 to α3 can affect the active-site directly, considering their locations near the entrance of the active site. The results demonstrate the possibility that low affinity ligand, such as halothane, can affect protein function through modulation of protein motions without causing significant alternation in the protein structure.

Halothane effects on the bound substrate

The binding to the active site by the enzymatic reaction product analog 19-NTHS has been well studied previously (7,30). Several lines of experimental evidence (7,30) suggest that Tyr-14 OH and Asp-99 COOH can provide hydrogen bonds to the oxygen of 19-NTHS, and this hydrogen bonding network has been confirmed computationally by an earlier 1.5-ns MD simulation (27). These important H-bonds were also observed in the present MD simulations. Throughout the simulation, however, halothane had no close contact with either Tyr-14 or Asp-99, both of which are believed to be critical for the substrate-KSI binding and for KSI enzymatic functions. Comparing to the much larger range of halothane movement in the active site free of 19-NTHS, the halothane molecule near the 19-NTHS-bound site (No. 4) in Fig. 1 *B* had much limited motion, both translational and rotational. The reduced free space in the 19-NTHS-bound site is partially responsible for the changes in halothane motion. More effective halothane interaction

with the adjacent residues, such as Asp-38, also contributes to more restricted halothane motion. The existence of halothane in the immediate vicinity of the bound 19-NTHS might help to stabilize this product analog in the active site. In contrast, the 19-NTHS in subunit B, where there was no halothane nearby, seemed to have a much stronger tendency to move out of the active site into the bulk water in the later stage of the MD simulation. The stabilization effect of halothane on the product analog 19-NTHS at the active site implies the possibility that due to the slower leaving of the product, KSI catalytic rate might slow down to some extent, which was indeed observed experimentally (10).

CONCLUSION

The anesthetic interference with enzymatic activities was previously interpreted as the results of competition for binding between anesthetic molecules and endogenous substrate at the substrate binding sites (31). Strong preference of halothane for the KSI dimer interface in this study suggests other possibilities for anesthetics to exert their action on proteins. At least two important conclusions can be drawn from this study: i), it is not necessary for anesthetic molecules to compete with substrate for the hydrophobic active-site cavity to exert an effect; and ii), anesthetic perturbation to the quaternary structure of a protein complex can be significant to the protein functions. The second conclusion is particularly important and can possibly be generalized, because quaternary structures are essential to multidomain receptors in the CNS, especially the Cys-loop receptors that have been identified as the potential targets for general anesthetics (1). What have been observed at the dimer interface of KSI, including the halothane interruption of the electrostatic interactions and bound water molecules between subunits, are also likely to occur in the Cys-loop receptors. Similarly, the consequences of anesthetic perturbation to the quaternary interaction in KSI, such as alternations in the motional characteristics of interfacial residues and other crucial residues within the loops, can also happen in the Cys-loop receptors. Therefore, the inferences from our study on KSI may prove highly relevant for the future investigations of anesthetic effect on the Cys-loop receptors, where similar and perhaps more intriguing anesthetic interaction components are involved.

SUPPLEMENTARY MATERIAL

An online supplement to this article can be found by visiting BJ Online at http://www.biophysj.org.

The authors thank Dr. Dejian Ma for stimulating discussion related to the NMR studies of KSI.

This research was facilitated through an allocation of advanced computing resources at the Pittsburgh Supercomputing Center through the support of the National Science Foundation and the Commonwealth of Pennsylvania. This research was supported in part by grants from the National Institutes of Health (R01GM066358, R01GM056257, and R37GM049202).

REFERENCES

1. Campagna, J. A., K. W. Miller, and S. A. Forman. 2003. Mechanisms of actions of inhaled anesthetics. *N. Engl. J. Med.* 348:2110–2124.
2. Franks, N. P., and W. R. Lieb. 2004. Seeing the light: protein theories of general anesthesia. 1984. *Anesthesiology.* 101:235–237.
3. Xu, Y., P. Tang, L. Firestone, and T. T. Zhang. 1996. 19F nuclear magnetic resonance investigation of stereoselective binding of isoflurane to bovine serum albumin. *Biophys. J.* 70:532–538.
4. Eckenhoff, R. G., C. E. Petersen, C. E. Ha, and N. V. Bhagavan. 2000. Inhaled anesthetic binding sites in human serum albumin. *J. Biol. Chem.* 275:30439–30444.
5. Kim, S. W., S. S. Cha, H. S. Cho, J. S. Kim, N. C. Ha, M. J. Cho, S. Joo, K. K. Kim, K. Y. Choi, and B. H. Oh. 1997. High-resolution crystal structures of delta5–3-ketosteroid isomerase with and without a reaction intermediate analogue. *Biochemistry.* 36:14030–14036.
6. Wu, Z. R., S. Ebrahimian, M. E. Zawrotny, L. D. Thornburg, G. C. Perez-Alvarado, P. Brothers, R. M. Pollack, and M. F. Summers. 1997. Solution structure of 3-oxo-delta5-steroid isomerase. *Science.* 276: 415–418.
7. Massiah, M. A., C. Abeygunawardana, A. G. Gittis, and A. S. Mildvan. 1998. Solution structure of Delta 5–3-ketosteroid isomerase complexed with the steroid 19-nortestosterone hemisuccinate. *Biochemistry.* 37: 14701–14712.
8. Kim, D. H., D. S. Jang, G. H. Nam, and K. Y. Choi. 2001. Folding mechanism of ketosteroid isomerase from Comamonas testosteroni. *Biochemistry.* 40:5011–5017.
9. Nam, G. H., D. H. Kim, N. C. Ha, S. Jang Do, Y. S. Yun, B. H. Hong, B. H. Oh, and K. Y. Choi. 2003. Contribution of conserved amino acids at the dimeric interface to the conformational stability and the structural integrity of the active site in ketosteroid isomerase from Pseudomonas putida biotype B. *J. Biochem.* (Tokyo). 134:101–110.
10. Yonkunas, M. J., D. Ma, Z. Liu, L. Li, Y. Xu, and P. Tang. 2004. Allosteric low-affinity drug action on ketosteroid isomerase. *Biophys. J.* 86:514a (Abstr.).
11. Morris, G. M., D. S. Goodsell, R. S. Halliday, R. Huey, W. E. Hart, R. K. Belew, and A. J. Olson. 1998. Automated docking using a Lamarckian genetic algorithm and an empirical binding free energy function. *J. Comput. Chem.* 19:1639–1662.
12. Tang, P., I. Zubryzcki, and Y. Xu. 2001. Ab initio calculation of structures and properties of halogenated general anesthetics: halothane and sevoflurane. *J. Comput. Chem.* 22:436–444.
13. Liu, Z. W., Y. Xu, A. C. Saladino, T. Wymore, and P. Tang. 2004. Parametrization of 2-bromo-2-chloro-1,1,1-trifluoroethane (halothane) and hexafluoroethane for nonbonded interactions. *J. Phys. Chem. A.* 108:781–786.
14. Hetenyi, C., and D. van der Spoel. 2002. Efficient docking of peptides to proteins without prior knowledge of the binding site. *Protein Sci.* 11:1729–1737.
15. Kale, L., R. Skeel, M. Bhandarkar, R. Brunner, A. Gursoy, N. Krawetz, J. Phillips, A. Shinozaki, K. Varadarajan, and K. Schulten. 1999. NAMD2: greater scalability for parallel molecular dynamics. *J. Comput. Phys.* 151:283–312.
16. Hoover, W. G. 1985. Canonical dynamics: equilibrium phase-space distributions. *Phys. Rev. A.* 31:1695–1697.
17. Humphrey, W., A. Dalke, and K. Schulten. 1996. VMD: visual molecular dynamics. *J. Mol. Graph.* 14:33–38.
18. Cho, H. S., G. Choi, K. Y. Choi, and B. H. Oh. 1998. Crystal structure and enzyme mechanism of Delta 5–3-ketosteroid isomerase from Pseudomonas testosteroni. *Biochemistry.* 37:8325–8330.
19. Kim, D. H., G. H. Nam, D. S. Jang, S. Yun, G. Choi, H. C. Lee, and K. Y. Choi. 2001. Roles of dimerization in folding and stability of

ketosteroid isomerase from Pseudomonas putida biotype B. *Protein Sci.* 10:741–752.

20. Otting, G., E. Liepinsh, B. T. Farmer 2nd, and K. Wuthrich. 1991. Protein hydration studied with homonuclear 3D 1H NMR experiments. *J. Biomol. NMR.* 1:209–215.
21. Halle, B., and V. P. Denisov. 2001. Magnetic relaxation dispersion studies of biomolecular solutions. *Methods Enzymol.* 338:178–201.
22. Ernst, J. A., R. T. Clubb, H. X. Zhou, A. M. Gronenborn, and G. M. Clore. 1995. Demonstration of positionally disordered water within a protein hydrophobic cavity by NMR. *Science.* 267:1813–1817.
23. Garcia, A. E., and G. Hummer. 2000. Water penetration and escape in proteins. *Proteins.* 38:261–272.
24. Sharrow, S. D., K. A. Edmonds, M. A. Goodman, M. V. Novotny, and M. J. Stone. 2005. Thermodynamic consequences of disrupting a water-mediated hydrogen bond network in a protein:pheromone complex. *Protein Sci.* 14:249–256.
25. Sharp, K. 2001. Entropy-enthalpy compensation: fact or artifact? *Protein Sci.* 10:661–667.
26. Park, H., and K. M. Merz, Jr. 2003. Molecular dynamics and quantum chemical studies on the catalytic mechanism of delta5–3-ketosteroid isomerase: the catalytic diad versus the cooperative hydrogen bond mechanism. *J. Am. Chem. Soc.* 125:901–911.
27. Mazumder, D., K. Kahn, and T. C. Bruice. 2003. Computational study of ketosteroid isomerase: insights from molecular dynamics simulation of enzyme bound substrate and intermediate. *J. Am. Chem. Soc.* 125:7553–7561.
28. Tang, P., P. K. Mandal, and M. Zegarra. 2002. Effects of volatile anesthetic on channel structure of gramicidin A. *Biophys. J.* 83:1413–1420.
29. Tang, P., and Y. Xu. 2002. Large-scale molecular dynamics simulations of general anesthetic effects on the ion channel in the fully hydrated membrane: the implication of molecular mechanisms of general anesthesia. *Proc. Natl. Acad. Sci. USA.* 99:16035–16040.
30. Cho, H. S., N. C. Ha, G. Choi, H. J. Kim, D. Lee, K. S. Oh, K. S. Kim, W. Lee, K. Y. Choi, and B. H. Oh. 1999. Crystal structure of delta(5)-3-ketosteroid isomerase from Pseudomonas testosteroni in complex with equilenin settles the correct hydrogen bonding scheme for transition state stabilization. *J. Biol. Chem.* 274:32863–32868.
31. Franks, N. P., and W. R. Lieb. 1984. Do general anesthetics act by competitive binding to specific receptors? *Nature.* 310:599–601.